Three-dimensional gas temperature measurements in atmospheric pressure microdischarges using Raman scattering

Sergey G. Belostotskiy, Qiang Wang, Vincent M. Donnelly,[a] and Demetre J. Economou[b]
Plasma Processing Laboratory, Department of Chemical and Biomolecular Engineering, University of Houston, Houston, Texas 77204-4004

Nader Sadeghi
Laboratoire de Spectrométrie Physique (UMR C5588), Université J. Fourier de Grenoble, BP 87, F-38402 Saint-Martin d'Hères Cedex, France

(Received 8 September 2006; accepted 6 November 2006; published online 21 December 2006)

Spatially resolved three-dimensional rotational Raman spectroscopy of ground state nitrogen was used to measure the gas temperature (T_g) in a normal dc glow microdischarge (300 μm gap between 0.5×0.05 mm^2 parallel electrodes) in pure N_2. An original backscattering confocal optical system with a spatial resolution of $\sim$40 μm was developed for collecting Raman spectra. Gas temperatures were measured at several points across the gap as well as along the axis perpendicular to the discharge plane. T_g peaked near the cathode and was 1200 K in the negative glow of a 500 Torr, 20 mA discharge. © *2006 American Institute of Physics*. [DOI: 10.1063/1.2404594]

High pressure nonequilibrium microdischarges have attracted much research in the past several years.[1–8] Due to their unique combination of small dimensions ($\sim$100 s of micrometers), atmospheric pressure operation, and high power densities (10–100 kW/cm^3), microdischarges find applications for excimer sources, sensors, plasma display panel cells, ozone sources, surface treatment, and biomedical processes.[3–5] Although these discharges operate in a glow (and not arc) mode, they can also be unstable and unpredictable. Thus, it is essential to measure and control basic plasma parameters. Unfortunately, the small size and high pressure preclude application of conventional diagnostics such as Langmuir probes and microwave interferometry.

This work introduces the application of Raman scattering for spatially resolved three-dimensional (3D) measurements of gas temperature (T_g) in nitrogen atmospheric pressure microdischarges. Gas temperature is an important parameter for microdischarges, since high power densities can result in considerable neutral gas heating with a concomitant reduction of the gas number density (N). This in turn affects the reduced electric field (E/N) in the plasma, and correspondingly all plasma parameters depending on E/N.

A schematic diagram of the experimental apparatus is presented in Fig. 1. A normal dc glow discharge in N_2 was ignited between two parallel molybdenum electrodes (gap between the electrodes $d=300$ μm, electrode surface area 5×0.5 mm^2). The discharge was operated at typical voltages of 360–400 V between the electrodes at currents of 5–30 mA. The chamber containing the microdischarge was evacuated, purged with N_2, and then sealed off at pressures of 400–700 Torr (i.e., no N_2 flowed during experiments). The microdischarge was mounted on a holder that was connected to an x-y-z linear stage (Newport, MFA Series). This arrangement allowed the discharge to be precisely moved with respect to the stationary laser beam and light collection optics, so that 3D spatially resolved measurements could be carried out.

The pulsed, frequency doubled Nd:YLF laser (Photonics Ind., DS10-527) had a wavelength of 526.5 nm, a spectral linewidth of 0.05 nm [full width at half maximum, (FWHM)], a pulse frequency of 3 kHz, a pulse duration of 100 ns, and an average power of 6 W. The laser beam was condensed with two lenses and guided into a periscope, which consisted of a Brewster's angle window, a right angle prism, and a 3 mm diameter, 15 mm focal length lens that focused the beam into the microdischarge. The cross section of the focused laser beam was close to a $\sim$40 μm FWHM Gaussian function. After passing between the electrodes, the laser beam was absorbed in a beam dump.

In most laser scattering experiments, light is detected at an angle of $\theta=90°$ with respect to the laser beam axis.[9–12] In a slot-type microdischarge with a long, deep, and narrow gap,[8] the axis perpendicular to the discharge plane (z axis, Fig. 4) is the only direction appropriate for a tightly focused laser beam. The same direction is also preferable for scattered light detection, since it provides the largest solid collection angle. Therefore, a backscattering geometry (i.e., $\theta=180°$) is more appropriate in such cases. This *confocal* arrangement is widely used in Raman microprobe measurements and in high-resolution optical microscopy.[13] In these cases, the laser beam and detected scattered light pass through the same lens, and the signal (at a sufficiently shifted wavelength) is split from scattered laser light with dichroic mirrors. In the present work, the extremely bright scattered light that would result from passing the laser beam through the collection lens, combined with the need to detect light very close to the laser wavelength, prevented use of the single lens arrangement. Consequently, the dual lens system depicted in Fig. 1 was used, with the laser passing through the small lens at the end of the periscope inside the chamber. Therefore, the laser beam did not pass through the objective lens and window used to view Raman scattering, minimizing background from scattering of the beam. The thin walls surrounding the small lens and prism minimized the light eclipsed by the end of the periscope, allowing 60% of the

[a]Electronic mail: vmdonnelly@uh.edu
[b]Electronic mail: economou@uh.edu

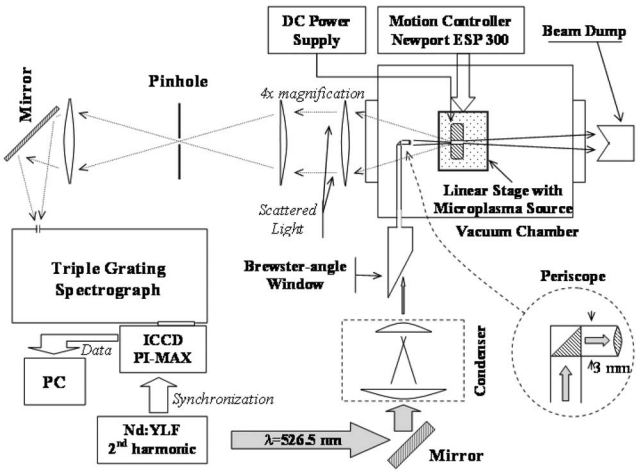

FIG. 1. Schematic diagram of the experimental apparatus for spatially resolved three-dimensional measurements of neutral gas temperature. The direction of the laser beam was perpendicular to the discharge plane (along the z axis, see Fig. 4).

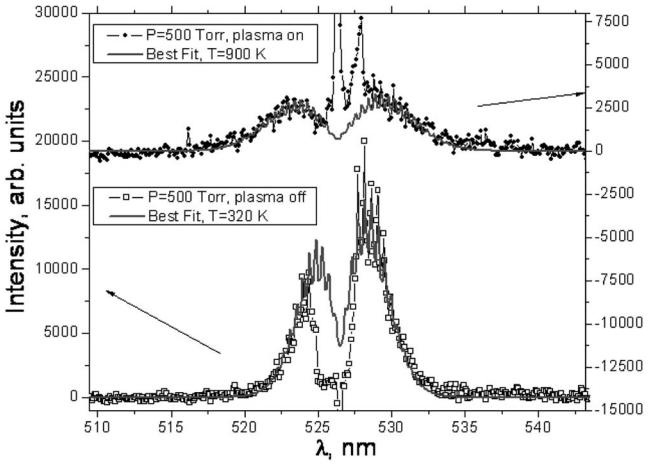

FIG. 2. (a) Examples of net (background subtracted) Raman spectra. (Top): Plasma on (p=500 Torr, I=20 mA), best fit T_g=900 K. (Bottom): Plasma off, best fit T_g=320 K (ambient temperature).

backscattered signal (that would be detected if the periscope could be removed) to be collected.

Scattered light was collected by two lenses and focused on a 100 μm diameter pinhole spatial filter with 4× magnification (Fig. 1). The transmitted light was then focused by a third lens (with 2× demagnification) onto the 100 μm entrance slit of the triple grating spectrometer (TGS). A detailed description of the TGS can be found in Refs. 10 and 11 Three flat holographic gratings (1200 grooves/mm) and six 20 cm focal length lenses were used, providing a dispersion of 3.5 nm/mm. The first grating dispersed the light, and the second grating recombined the dispersed light. A spatial filter at the focal plane between the two gratings blocked the laser wavelength. Different combinations of spatial filters and entrance slits were evaluated for rejecting scattered laser light, while maintaining an adequate portion of the Raman spectrum with sufficient resolution. The optimum performance was found to be a 100 μm slit width and a 750 μm wide spatial filter. With the laser scattered light reduced by a factor $\sim 10^4$, the third grating dispersed the light over 10.9 pixels/nm on an intensified charge-coupled device (ICCD, Princeton Instruments model PI-MAX). The ICCD was gated on for 300 ns, synchronized with the laser pulse, to reject most of the background emission from the plasma.

Spectra accumulated over typically 100 s (3×10^5 laser pulses) were recorded on a computer and processed by a program that implemented a nonlinear least squares fit to the experimental data. The synthetic spectra were a convolution of the theoretical Raman spectrum (100 rotational levels of N_2 were accounted for) with the measured apparatus function.[10,14] Since the laser linewidth is much smaller than the TGS resolution (0.35 nm FWHM with a 100 μm entrance slit width), the apparatus function is mainly represented by a 0.35 nm FWHM Gaussian function. By observing the laser line (without the spatial filter), it was found that a second, broad Gaussian function (2.7 nm FWHM) was also required to account for a relatively small background, perhaps from scattering off the optics or the face of the ICCD.

Figure 2 presents typical net (with the background subtracted) spectra recorded with the plasma on (top) and off (bottom). The gas temperature was determined from the best synthetic fit to the observed spectrum, with T_g as the adjustable parameter. The background-dominated region close to the laser wavelength was excluded from the fit. The net spectrum with the plasma off was fit first to obtain the proportionality constant relating the measured signal intensity to the relative computed intensity. This also confirmed that the model correctly predicted the gas temperature which, with the plasma off, was the ambient temperature. The same proportionality constant was then used to fit spectra recorded with the plasma on. The good fit to the observed plasma-on spectrum showed that N_2 was the dominant species with a number density that varied as $1/T_g$ at constant pressure, as expected.

Using this approach, spatially resolved T_g profiles of N_2 dc microdischarges were obtained. An example of measurements along the axis perpendicular to the discharge plane (z axis) is presented in Fig. 3 (left). Measurements across the gap (x axis, see Fig. 4) are given in Fig. 3 (right). As expected, T_g drastically increases in the region between the electrodes, where the plasma was sustained and power dissipation occurs (Fig. 3, left). The difference in T_g above and

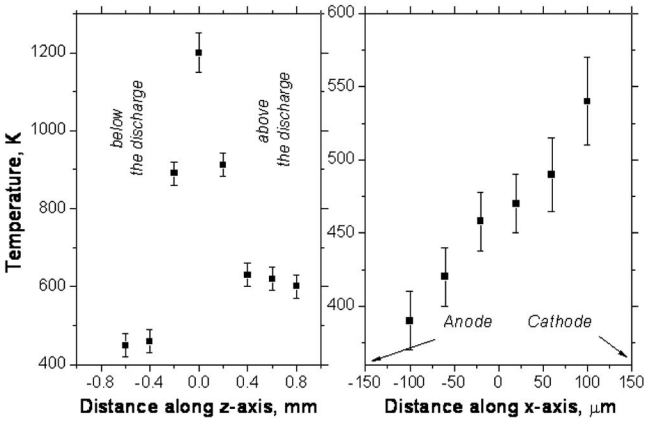

FIG. 3. Examples of spatially resolved gas temperature in a N_2 dc microdischarge at p=500 Torr and I=20 mA. (Left): Measurements along the z axis (see Fig. 4) perpendicular to the plane of the discharge. z=0 corresponds to the negative glow region (x=100 μm). (Right): Measurements across the discharge gap (x axis, see Fig. 4) at an elevation of 0.8 mm above the plasma center (z=0.8 mm). x=−150 and 150 μm correspond to the location of the anode and cathode, respectively.

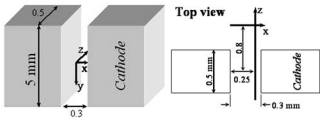

FIG. 4. Schematic of the discharge geometry showing the scan directions along the *x*-axis and *z*-axis (all dimensions are in mm).

below the plasma may be due to the metal holder which, acting as a heat sink, can cool the gas below the discharge. The data in Fig. 3 (right), collected above the plasma region ($z=0.8$ mm), are typical for dc discharges.[8] Since power is mainly dissipated in the cathode region (due to the high electric field in that region) T_g near the cathode is higher than the rest of the microdischarge.

In summary, Raman scattering was employed for spatially resolved three-dimensional measurements of gas temperature in nitrogen dc glow microdischarges. An original confocal microscope arrangement allowed a spatial resolution of ~ 40 μm. Scattered radiation was observed using a backscattering geometry. The measured spatial temperature profiles reflect the basic features of dc microdischarges. For a 500 Torr, 20 mA microdischarge, the gas temperature T_g peaked at ~ 1200 K in the negative glow of the microdischarge. Scans across the discharge gap revealed that T_g was highest near the cathode.

The authors thank the Department of Energy (Grant No. DE-FG02-03ER54713) for funding this work and A. Kono of Nagoya University for help with the design of TGS. One of the authors (S.B.) greatly appreciates the recommendations of Dmitry Lopaev and Vladimir Pirogov from Moscow State University concerning aspects of optics and laser spectroscopy.

[1] K. H. Becker, K. H. Schoenbach, and J. G. Eden, J. Phys. D **39**, R55 (2006).
[2] M. Kushner, J. Phys. D **38**, 1633 (2005).
[3] U. Kogelschatz, Plasma Phys. Controlled Fusion **46**, B63 (2004).
[4] J. P. Boeuf, J. Phys. D **36**, R53 (2003).
[5] R. E. J. Sladek and E. Stoffels, J. Phys. D **38**, 1716 (2005).
[6] C. G. Wilson, Y. B. Gianchandani, R. R. Arslanbekov, V. Kolobov, and A. E. Went, J. Appl. Phys. **94**, 2845 (2003).
[7] V. I. Arkhipenko, A. A. Kirillov, L. V. Simonchik, and S. M. Zgirouski, Plasma Sources Sci. Technol. **14**, 757 (2005).
[8] Q. Wang, I. Koleva, V. M. Donnelly, and D. J. Economou, J. Phys. D **38**, 1690 (2005).
[9] M. J. van de Sande and J. J. A. M. van der Mullen, J. Phys. D **35**, 1381 (2002).
[10] M. J. van de Sande, Ph.D. Thesis, Eindhoven University of Technology, The Netherlands, 2002; http://alexandria.tue.nl/extra2/200210414.pdf
[11] A. Kono and K. Nakatani, Rev. Sci. Instrum. **71**, 2716 (2000).
[12] K. Muraoka, K. Uchino, and M. D. Bowden, Plasma Phys. Controlled Fusion **40**, 1221 (1998).
[13] W. Demtroder, *Laser Spectroscopy: Basic Concepts and Instrumentation*, 2nd ed. (Springer, Berlin, 1996), p. 834.
[14] D. A. Long, *Raman Spectroscopy* (McGraw-Hill, New York, 1977).